

RESEARCH ARTICLE

Disposition and metabolism of LY2603618, a Chk-1 inhibitor following intravenous administration in patients with advanced and/or metastatic solid tumors

Enaksha R. Wickremsinhe¹, Scott M. Hynes¹, Margo D. Palmieri¹, Malcolm I. Mitchell², Trent L. Abraham¹, Jessica Fayer Rehmel¹, Emilie Chana², Lorenz M. Jost³, and Kenneth C. Cassidy¹

¹Lilly Research Laboratories, Eli Lilly and Company, Indianapolis, IN, USA, ²Eli Lilly and Company, Erl Wood Manor, Windlesham, Surrey, UK, and

³Kantonsspital Baselland-Bruderholz, Oncology Department, Bruderholz, Switzerland

Abstract

1. The disposition and metabolism of a Chk-1 inhibitor (LY2603618) was characterized following a 1-h intravenous administration of a single 250-mg dose of [¹⁴C]LY2603618 (50 μCi) to patients with advanced or metastatic solid tumors.
2. LY2603618 was well tolerated with no clinically significant adverse events. Study was limited to three patients due to challenges of conducting ADME studies in patients with advanced cancer. Plasma, urine and feces were analyzed for radioactivity, LY2603618 and metabolites. LY2603618 had a half-life of 10.5 h and was the most abundant entity in plasma, accounting for approximately 69% of total plasma radioactivity. The second most abundant metabolites, H2 and H5, accounted for <10% of total circulating radioactivity. The major route of clearance was via CYP450 metabolism. The mean total recovery of radioactivity was 83%, with approximately 72% of the radioactivity recovered in the feces and approximately 11% in the urine. LY2603618 represented approximately 6% and 3% of the administered dose in feces and urine, respectively.
3. A total of 12 metabolites were identified. *In vitro* phenotyping indicated that CYP3A4 was predominantly responsible for the metabolic clearance of LY2603618. Additionally, aldehyde oxidase was involved in the formation of a unique human and non-human primate metabolite, H5.

Keywords

Aldehyde oxidase, cancer patients, excretion, mass balance, radiolabelled study

History

Received 24 January 2014
Revised 27 February 2014
Accepted 28 February 2014
Published online 26 March 2014

Introduction

LY2603618 (1-{5-bromo-4-methyl-2-[(2s)-morpholin-2-ylmethoxy]phenyl}-3-(5-methylpyrazin-2-yl)urea) is a potent and selective inhibitor of the deoxyribonucleic acid (DNA) damage checkpoint kinase one (Chk-1; Matthews et al., 2013). Based on non-clinical efficacy studies *in vitro* and *in vivo*, LY2603618 enhances the activity of chemotherapeutic agents but has little effect on tumor cells on its own (as a single agent; King et al., 2014). In animal xenograft tumor studies, LY2603618 in combination with chemotherapy agents resulted in greater tumor reduction than chemotherapy agents alone. LY2603618 is being studied in combination with either gemcitabine or pemetrexed/cisplatin (Weiss et al., 2013).

Radiolabelled disposition studies are conducted as part of the new drug development process to understand the mass balance, and routes of excretion, and to identify metabolites and metabolic pathways (Penner et al., 2009; Roffey et al., 2007). Typically, these studies are conducted using healthy volunteers; however, the cytostatic properties of LY2603618 combined with cytotoxic DNA-damaging chemotherapeutic agents, such as gemcitabine or pemetrexed, precluded the possibility of conducting the study in a healthy volunteer population. Conducting radiolabelled disposition studies in oncology patients is challenging due to issues related to patient enrolment as well as overall study administration and conduct, especially pertaining to dosing and handling of radiolabelled drug and sample collection. This study was conducted to determine the disposition and metabolism of radioactivity and LY2603618 in patients with advanced or metastatic solid tumors after intravenous (IV) administration of a single 250-mg dose of [¹⁴C]LY2603618 (~50 μCi or 1.85 megabecquerel [MBq]). In addition, *in vitro* experiments were conducted to estimate the fraction of cytochrome P450 (CYP450)-mediated clearance by individual P450s and to identify and understand the unique human metabolite and non-human primate, H5.

Address for correspondence: Enaksha Wickremsinhe, PhD, Principal Research Scientist, Lilly Research Laboratories, Eli Lilly and Company, Indianapolis, Indiana 46285, USA. Tel: +1 317-433-9290. Fax: +1 317-433-6432. E-mail: enaksha@lilly.com

Materials and methods

Reference compounds

LY2603618, [¹⁴C]LY2603618 (uniformly labelled on the bromo-phenyl ring) and [D₅]-LY2603618 (used as internal standard for liquid chromatography–mass spectrometry [LC–MS] analysis) were obtained from Eli Lilly and Co, Indianapolis, IN.

Study design and patients

This was a single-centre, open-label study in which patients with advanced or metastatic solid tumors received a single IV dose of 250-mg LY2603618 containing [¹⁴C]LY2603618 (50 μCi), as Cycle 1. The study was conducted in Switzerland at the Kantonsspital Bruderholz, Oncology Department, Bruderholz, Switzerland. After a minimum 7-day washout to complete the ¹⁴C phase of the study, patients were allowed to continue dosing with LY2603618, in combination with either gemcitabine or pemetrexed (Cycles 2 and beyond). The continued access portion of the study provided the opportunity for patients to receive LY2603618 in combination with gemcitabine or pemetrexed as a possible treatment option, as determined by the investigator.

The protocol was reviewed and approved by the Ethikkommission beider Basel ERB in Basel, Switzerland. The study was conducted in accordance with the ethical principles stated in the Declaration of Helsinki. All patients provided written informed consent prior to entering the study. The study was registered on clinicaltrials.gov (NCT01296568).

Patients were at least 18 years of age, male or female, with a body surface area $\geq 1.37 \text{ m}^2$, who had a histological or cytological diagnosis of cancer (solid tumor), with clinical or radiologic evidence of locally advanced and/or metastatic disease for which no life-prolonging therapy exists. Patients were admitted to the Clinical Research Unit (CRU) on the day prior to dosing (Day –1). The first two patients remained at the CRU for approximately 7 days post-dose, and the third patient remained at the CRU for approximately 5 days post-dose; during which samples were collected for the determination of total radioactivity and plasma concentrations of LY2603618. Requiring patients to remain resident in the clinic for long periods of time was a deterrent to enrolling patients. The quick-count data from the first two patients enrolled showed that greater than 80% of the administered radioactivity was excreted by the 96-h time point. Therefore, the study protocol was amended after the first two patients to allow the release of patients following the 96-h time point collections.

For patients who participated in the combination treatment period, a follow-up assessment was performed approximately 7–21 days after the planned end of the last period.

This study was not designed to test efficacy; however, the objective response outcome of patients receiving LY2603618 in combination with gemcitabine or pemetrexed using Response Evaluation Criteria In Solid Tumors (RECIST: version 1.1) criteria was collected during the continued access phase. For purposes of collecting objective response, tumor assessments were compared to the screening tumor

assessment as a baseline. The planned duration of treatment was not fixed; patients remained in the study until the patient or attending physician requested the patient be withdrawn due to disease progression; any ethical, medical or scientific reason, while considering the rights, safety and well-being of the patient; or the patient's experience of unacceptable toxicity.

Drug administration

[¹⁴C]LY2603618 was supplied by Eli Lilly and Company as a 20-mL vial containing 250-mg LY2603618 formulated as a frozen solution, which was thawed prior to removal of the dose for further dilution in 5% dextrose in water (D5W). The [¹⁴C]LY2603618 single IV dose was administered on Day 1 of Cycle 1. The entire IV dose was administered to the patient over 1 hour. [¹⁴C]LY2603618 was stored at –15 to –25 °C. Completion of Cycle 1 constituted the end of the disposition part of the study. The [¹⁴C]LY2603618 was manufactured and tested in accordance with Good Manufacturing Practice standards. LY2603618 (provided by Eli Lilly) was provided to patients starting from Cycle 2 for administration during the continued access phase of the study. The three patients enrolled in this study received gemcitabine plus LY2603618 during the continued access phase (Cycle 2 and beyond). Gemcitabine was administered over approximately 30 min at a dose of 1000 mg/m² on Days 1, 8 and 15 of a 28-day cycle. Approximately 24 h after gemcitabine administration, a flat dose of 230 mg of LY2603618 was administered as an IV infusion (on Days 2, 9 and 16). Gemcitabine was stored at 10–25 °C.

Sample collection

Venous blood samples of approximately 8 mL each were drawn in to lithium heparin vacutainers to measure concentrations of radioactivity in blood and plasma and for the determination of the plasma concentrations of LY2603618 (pharmacokinetic [PK] samples). Blood and plasma samples were collected pre-dose, at 0.5, 1, 2, 4, 6, 8, 12 and 24 h post-dose (post-dose time points were measured from the start of infusion; therefore, 0.5 h was the mid-point of the infusion, and 1 h was the end of the infusion); and then at 24-h intervals until discharge criteria were met. Urine samples were collected at 0–6, 6–12, 12–24 h post-dose and then at 24-hour intervals until the discharge criteria were met. Feces were collected at 24-h intervals until discharge criteria were met. Expired air was sampled at 1, 2, 4, 8 and 24 h and then at 24-h intervals by blowing into an aliquot of trapping solution for 2 min, until the discharge criteria were met. Additional venous blood samples of approximately 8 mL each were drawn in to lithium heparin vacutainers for plasma metabolite profiling at 1, 2, 4, 8, 24 and 72 h post-dose.

Measurement of total radioactivity

Whole blood, plasma, urine, fecal and expired air concentrations of total radioactivity were determined using liquid scintillation counting techniques. All sample combustions were performed using a Model 307M Sample Oxidizer (Perkin Elmer), and the resulting ¹⁴CO₂ was trapped in a mixture of Carbo Sorb E and Perma Fluor E+ (Perkin Elmer,

Waltham, MA). Fecal samples (~0.4 g) were combusted and analyzed in duplicate. Blood samples (~0.4 g) were combusted and analyzed in duplicate. Plasma (~0.2 g) and urine samples (~1 g) were analyzed in duplicate. The amount of drug excreted in feces, urine, and expired air and the fraction of the dose excreted in feces, urine and expired air was determined. The radioanalysis portion of this study was conducted at Covance Laboratories Limited, North Yorkshire, UK. Quantification of air samples was performed at Harlan Laboratories Ltd, Itingen, Switzerland.

Pharmacokinetic analysis

The samples were analyzed for LY2603618 on a Sciex API 3000 using a TurboIonSpray in positive ionization mode. LY2603618 and the internal standard were isolated from 50 μ L of lithium heparinized human plasma using a protein-precipitation extraction procedure. Chromatography was performed using a gradient consisting of 0.05% formic acid in water as mobile phase A and acetonitrile using a Hypersil Gold C₁₈ (2.1 \times 50 mm, 5- μ m) high-performance liquid chromatography (HPLC) column at 300 μ L/min. Selected Reaction Monitoring was used following the transition of m/z 436.1 \rightarrow 301.1 for LY2603618 and m/z 441.1 \rightarrow 306.1 for its stable-labelled internal standard. The lower limit of quantitation was 2 ng/mL, and the upper limit of quantitation was 500 ng/mL. Plasma samples were analyzed at Quintiles (Ithaca, NY).

The PK parameters of LY2603618 were determined based on the LY2603618 concentrations in plasma. In addition, PK parameters were also calculated for the total radioactivity in whole blood and plasma, using a non-compartmental method of analysis with WinNonlin Professional Version 5.2 (Pharsight, Sunnyvale, CA). The following PK parameters were determined: area under the concentration versus time curve (AUC) from time zero to time t , where t is the last time point with a measurable concentration (AUC[0- t_{last}]); AUC from time zero to infinity (AUC[0- ∞]); fraction of AUC(0- ∞) extrapolated (%AUC[t_{last} - ∞]); maximum observed drug concentration (C_{max}); time of maximum observed drug concentration (t_{max}); last time point, where the concentration is above the limit of quantitation (t_{last}); apparent plasma terminal elimination half-life ($t_{1/2}$); total body clearance of drug (LY2603618 only) calculated after IV administration (CL); and volume of distribution during the terminal phase (LY2603618 only; V_z).

Sample preparation for metabolite profiling and identification

Plasma samples were precipitated with acetonitrile followed by centrifugation. Extraction of protein pellets was repeated and the supernatants combined, evaporated to dryness, and then reconstituted in an appropriate volume of 20/80 0.2% formic acid/methanol to give a final concentration factor of 10 times the original volume. The extraction efficiencies ranged from 77% to 100%.

Urine samples from 0 to 6, 6 to 12 and 12 to 24 h were pooled within patients. Aliquots were loaded on a preconditioned Biotage Isolute C18 SPE cartridge (Biotage, Charlotte, NC). The cartridges were preconditioned by washing with

methanol followed by 0.2% formic acid. After loading, cartridges were washed with 0.2% formic acid and eluted with methanol. The eluents were evaporated to dryness and reconstituted in 70/30 0.2% formic acid/methanol to give a final 10-fold concentration. The mean extraction efficiency of radioactivity from urine was calculated to be 94%.

Feces samples were pooled across 24–72 h time points within patients. The 72–96 h sample was extracted directly. Aliquots of fecal homogenates were extracted with acetonitrile/methanol/0.2% formic acid (35:35:30, v/v/v) three times; the supernatants were combined, evaporated to dryness and reconstituted in 60% (50:50 acetonitrile:methanol + 5% DMSO): 40% (0.2% formic acid). The mean extraction efficiency of radioactivity from feces was 97%. The metabolism portion of this study was conducted at Quintiles (Plainfield, IN).

Metabolite radioprofiling by HPLC

Metabolites in the various matrices were separated on a reverse-phase HPLC column (Synergi Polar RP, 4.6 mm \times 250 cm, 4 μ m, Phenomenex, Torrance, CA). Mobile phase A was 0.2% (v/v) aqueous formic acid, and mobile phase B was methanol with the following gradient: 0–3 min held at 30% B; 3–10 min linear gradient to 50% B; 10–20 min held at 50% B; 20–45 min linear gradient to 70% B; 45–65 min linear gradient to 90% B. A secondary method (Luna Phenyl Hexyl, 4.6 mm \times 250 cm, 5 μ m, Phenomenex, Torrance, CA) used for the separation of H1 and H2 metabolites used the following gradient: 0–3 min held at 10% B; 3–20 min linear gradient to 15% B; 20–60 min linear gradient to 30% B. For both methods, the total HPLC flow rate was 1 mL/min, with a post-column split so that approximately 20% of the total flow was introduced to the LC–MS interface, and the remaining flow was collected for radioprofiling. Radioprofiles of various matrix extracts were generated by HPLC fraction collection followed by off-line radioactivity counting. HPLC column effluent was collected into four 96-well LumaPlates (Perkin Elmer, Waltham, MA) at 12-s intervals. The plates were dried under centrifugal vacuum, counted for radioactivity on a TopCount NXT (Perkin Elmer, Waltham, MA) counter (5 min per well) and plotted and integrated using Perkin Elmer ProFSA software (Perkin Elmer, Waltham, MA). Chromatographic peaks below 7 cpm (plasma and urine) and 15 cpm (feces) were not integrated for peak areas. Each integrated peak was expressed as % region of interest (ROI), and all integrated peaks together constituted 100% ROI. The analysis was conducted at Quintiles (Plainfield, IN).

Structural characterization of metabolites by LC–MS

High resolution LC–MS and LC–MS/MS on a ThermoFinnigan LTQ Orbitrap (ThermoFinnigan, Waltham MA) were used for metabolite identification. Analysis was conducted in positive ion electrospray mode with a source voltage of 4.5 kV, capillary temperature of 350 $^{\circ}$ C and the resolution set at 30 000. MS–MS was conducted with higher energy collision dissociation (HCD) and collision energy of 45%. Analysis was performed by Quintiles (Plainfield, IN).

Structural characterization by NMR

Nuclear magnetic resonance (NMR) experiments were performed on a Varian 500NMR (Agilent Technologies, Santa Clara, CA) instrument with field strength of 11.7 T. The probe was a Varian gradient, triple resonance, Xsens cold probe. All analytes were dissolved in CD₃OD, and the experiments were conducted at 25 °C. Proton, gCOSY (correlation spectroscopy), gc2hsqc and gHMBCAD (metabolite H2 only) were used. Spectra were referenced with respect to solvent signal at 3.31 ppm for ¹H and 49.5 ppm for ¹³C.

Metabolite H2 and H3 generation in liver microsomes

Human, primate and dog liver microsome (XenoTech LLC, Lenexa, KS) incubations were conducted in two 96-well polypropylene plates. Incubation mixtures were composed of 100 mM sodium phosphate buffer (pH 7.4), containing 5 mM magnesium chloride and 1 mg/mL microsomal protein. The mixtures were pre-warmed for 3 min, NADPH (Sigma-Aldrich, St. Louis, MO) added to give a 2 mM final concentration to initiate the reaction, and incubated in a shaking water bath at approximately 37 °C for 3 h. Incubations for the isolation of H3 were quenched by adding an equal volume of acetonitrile, centrifuged and the supernatants pooled. Incubations for the isolation of H2 were quenched with 30% formic acid, vortex mixed, centrifuged and the supernatant transferred to a conical-bottom polypropylene tube. The respective pellets were re-extracted and the supernatant fractions combined.

The pooled supernatant for H3 isolation and the pooled supernatant for H2 isolation were evaporated to a volume of approximately 5 mL under a stream of nitrogen in a water bath at 45 °C for approximately 8 h, then cooled to approximately 20 °C for overnight drying. Each concentrated supernatant was chromatographed on a 10 × 250 mm Xbridge C18 column, 5 micron (Waters, Milford, MA). A linear mobile phase gradient of 10 mM ammonium bicarbonate and methanol was used. Fractions of the column effluent were collected in 15-s intervals and analyzed by off-line LC–MS. Fractions that contained H3 or H2 were pooled and evaporated to dryness as described above. The dry residue containing H3 was submitted for NMR analysis. The concentrated pool containing H2 was chromatographed again on an Xbridge C18 semi-preparative column; at this time, a linear mobile phase gradient of 10 mM ammonium formate and acetonitrile was used. Fractions were collected and analyzed by LC–MS. Fractions containing H2 were pooled, the solvent was completely evaporated as described above, and the residue was submitted for NMR analysis.

Characterization of enzyme responsible in the formation of H5

LY2603618 was incubated at 10 μM in Sprague–Dawley rat, Beagle dog, Cynomolgus monkey and human liver cytosol and microsomes (XenoTech LLC, Lenexa, KS). Cytosol incubations were in uncapped glass scintillation vials (20 mL) at a volume of 5 mL, including 500 μL of cytosol, in a CO₂ incubator (5% CO₂) on an orbital shaker (at 100 rpm and 37 °C) for up to 24 h. Liver microsome incubations were in

uncapped 2 mL polypropylene vials at a volume of 1 mL, 1 mg/mL protein, in a shaking water bath at 37 °C. The reaction was initiated with the addition of NADPH (2 mM final concentration). Aliquots of liver cytosol or microsome incubations were removed after 1 and 3 h quenched by adding an equal volume of acetonitrile, transferred to microcentrifuge tubes and centrifuged. The supernatant was analyzed by LC–MS for the detection and identification of H5, H3 and H2.

Additional incubations were performed to investigate the effects of hydralazine (Selleck Chemical LLC, Radnor, PA), a known inhibitor of aldehyde oxidase (AO), on the formation of H5 in human liver cytosol. Ten incubations, scaled down to 1 mL each, were conducted as described above, and a final concentration of 100 μM hydralazine was added to 5 of them. After quenching and centrifugation, the supernatant was analyzed by LC–MS for H5.

Identification of cytochromes P450 metabolizing LY2603618 with prediction of contributions to hepatic CYP-mediated clearance

Identification of P450s and quantitative predictions were performed as outlined in Rehm et al. (2012). Human liver microsomes (HLMs) from a mixed-gender pool of 150 individuals were purchased from BD Biosciences (Woburn, MA). Recombinant P450 enzymes (rCYP1A2, rCYP2B6, rCYP2C8, rCYP2C9, rCYP2C19, rCYP2D6, rCYP2E1, rCYP2J2, rCYP3A4 and rCYP3A5), provided as SupersomesTM (microsomes prepared from insect cells engineered to overexpress cDNA for human CYPs and reductase) and membrane control (microsomes prepared from baculovirus empty vector infected insect cells) were also purchased from BD Biosciences (Woburn, MA).

Stock solutions of 1 mM LY2603618 in methanol and 1 mM verapamil (Sigma–Aldrich, St. Louis, MO) in acetonitrile were prepared. LY2603618 was incubated in triplicate at 30 and 300 nM, and verapamil (positive control) was incubated in duplicate at 300 nM. About 100 μL aliquots containing LY2603618 or verapamil (1% final solvent concentration) and each matrix at 0.25 mg/mL in 100 mM sodium phosphate buffer (pH 7.4) were pre-warmed for 3 min at 37 °C. Reactions (at 37 °C) were started with the addition of NADPH (1 mM final concentration) and quenched at 5 and 30 min by the addition of 100 μL acetonitrile (5- and 30-min incubations were conducted in separate 96-well plates). The plates were centrifuged, and the supernatants were further processed using a 1:1 dilution with internal standard in water:acetonitrile (50:50; v:v). Samples were analyzed by LC–MS/MS. According to the screening set results, rCYP3A4 required further optimization to obtain first-order kinetics. Optimized conditions for rCYP3A4 were as noted above except incubation times were 15 and 30 min, and LY2603618 concentrations were 30 and 60 nM. A multifactorial approach ensured that valid signals were identified. First, rCYPs exhibiting ≥15% depletion were identified, then further evaluations were made for time-dependent depletion. Statistical analysis was conducted in SAS JMP, version 9.0.2 (SAS Institute Inc., Cary, NC). Replicate concentration data (at each of the different combinations of incubation

Table 1. Baseline characteristics of enrolled patients.

Patient Number	Age (years)	Sex	Race	Diagnosis of Cancer	Weight ^a (kg)	Height (cm)	BMI (kg/m ²)	ECOG PS ^b
1001	63	F	White	Epithelial ovarian cancer, endometrioid adenocarcinoma	54.2	158.0	21.7	0
1002	70	F	White	Lung cancer, adenocarcinoma	73.7	170.0	25.5	0
1003	56	M	White	Undifferentiated non-small-cell lung cancer, probable adenocarcinoma	63.5	160.0	24.8	1

F = female; M = male; BMI = body mass index; ECOG PS = Eastern Cooperative Oncology Group Performance Status.

^aScreening weight.

^bECOG PS at screening: 0 = Fully active, able to carry on all pre-disease performance without restriction; 1 = Restricted in physically strenuous activity but ambulatory and able to carry out work of a light or sedentary nature, e.g. light house work, office work.

times and concentrations) were natural log-transformed and analyzed by analysis of variance with Dunnett's test for differences from membrane control with $p \leq 0.05$. Intrinsic clearance (CL_{int}) of substrate depletion was calculated as:

$$CL_{int} = k_{dep} \times \frac{\text{Incubation volume}}{\text{pmol rCYP}} \quad (1)$$

where k_{dep} is the substrate depletion rate constant determined by calculating the slope from time (min) and natural log (ln) % of control remaining data using the LINEST function in Excel and pmol rCYP obtained by using lot-specific rCYP content (pmol \times mg protein⁻¹). To predict fm_{CYP} from the CL_{int} values, a relative activity factor (RAF)-based scaling approach was applied to generate scaled HLM CL_{int} (Nakajima et al., 1999). All HLM CL_{int} values were summed, and the fraction metabolized by a particular CYP (f_m) was determined. The depletion rate constant (k) for each rCYP was determined relative to the membrane control (k_{dep} = slope of time versus % ln remaining activity) and used to calculate rCYP intrinsic clearance (per pmol; CL_{int} ($\mu\text{L} \times \text{min}^{-1} \times \text{pmol}^{-1}$) by Equation (1). Scaled HLM CL_{int} CYP was predicted by multiplying rCYP CL_{int} by a predetermined RAF as in Rehm et al. (2012). Incubations, LC-MS/MS analysis, and data handling were performed by Quintiles (Plainfield, IN).

Conservative static model-based estimation of the magnitude of potential drug-drug interactions upon inhibition of CYP-mediated clearance of LY2603618

The fraction LY2603618 cleared via CYPs (F_{m,all_CYPs}) was determined by the following equation:

$$F_{m,all_CYPs} = 1 - (F_{e,parent} + F_{m,AO}) \quad (2)$$

where $F_{e,parent}$ represents the fraction of [¹⁴C]LY2603618 eliminated unchanged in the urine and faeces, and $F_{m,AO}$ represents the fraction of [¹⁴C]LY2603618 that could be definitively assigned as being eliminated by AO.

The effect of complete inhibition of clearance of LY2603618 by CYPs was estimated as follows:

$$\frac{AUC_i}{AUC} = \frac{1}{(1 - f_{m,all_CYPs})} \quad (3)$$

where AUC_i is the area under the curve in the inhibited state.

Results

Patient enrolment

A total of three patients, one male and two female between the ages of 56 and 70 years participated in this study (Table 1). All three patients received a single dose of [¹⁴C]LY2603618 on Day 1/Cycle 1 and completed the disposition phase of the study (Cycle 1). The time span between the dosing of the first patient and the last (third) patient was approximately 10 months, while the duration between the manufacture of the [¹⁴C]LY2603618 drug product and dosing of the last patient was approximately 15 months. Drug product stability data for [¹⁴C]LY2603618 was generated covering a period of approximately 19 months to enable dosing over this extended period of time, counting from the day of manufacture.

All three patients continued on to the continued access phase (Cycles 2 and beyond) with combination therapy with gemcitabine and completed at least one cycle of the continued access phase prior to being withdrawn from the study. The first patient was diagnosed with Stage III epithelial adenocarcinoma and endometrioid ovarian. The patient received her last dose of LY2603618 on Day 2/Cycle 3. The patient was lost to follow-up and was discontinued on Day 9/Cycle 3. The second patient was diagnosed with metastatic lung adenocarcinoma. This patient received her last dose of LY2603618 on Day 9/Cycle 5 and was discontinued on Day 52/Cycle 5 due to progressive disease. The third patient was diagnosed with Stage IV bronchial carcinoma. This patient received his last dose of LY2603618 on Day 9/Cycle 3. The patient decided to leave the study and was discontinued on Day 15/Cycle 3. LY2603618 was well tolerated in patients with no adverse events greater than grade 1 when administered as a solo agent.

Pharmacokinetics of LY2603618 and total radioactivity

Two patients received a dose of approximately 250-mg of [¹⁴C]LY2603618 containing approximately 1.85 MBq of radioactivity, and one patient received 240 mg of [¹⁴C]LY2603618 containing approximately 1.78 MBq of radioactivity, administered as an IV dose over approximately 1 h. The start and stop times were recorded for doses containing [¹⁴C]LY2603618 (Cycle 1), allowing for the accurate calculation of the doses administered. On Day 1/Cycle 1, the end of the infusion blood samples were taken approximately 5–15 min after the end of the infusion rather than immediately prior to end of infusion.

Figure 1. Arithmetic mean (\pm SD) concentration profiles vs time representing LY2603618 in plasma, total radioactivity in plasma and total radioactivity in blood following a single IV administration of [14 C]LY2603618 to patients ($N=3$). Inset shows magnified view of 0–12 h.

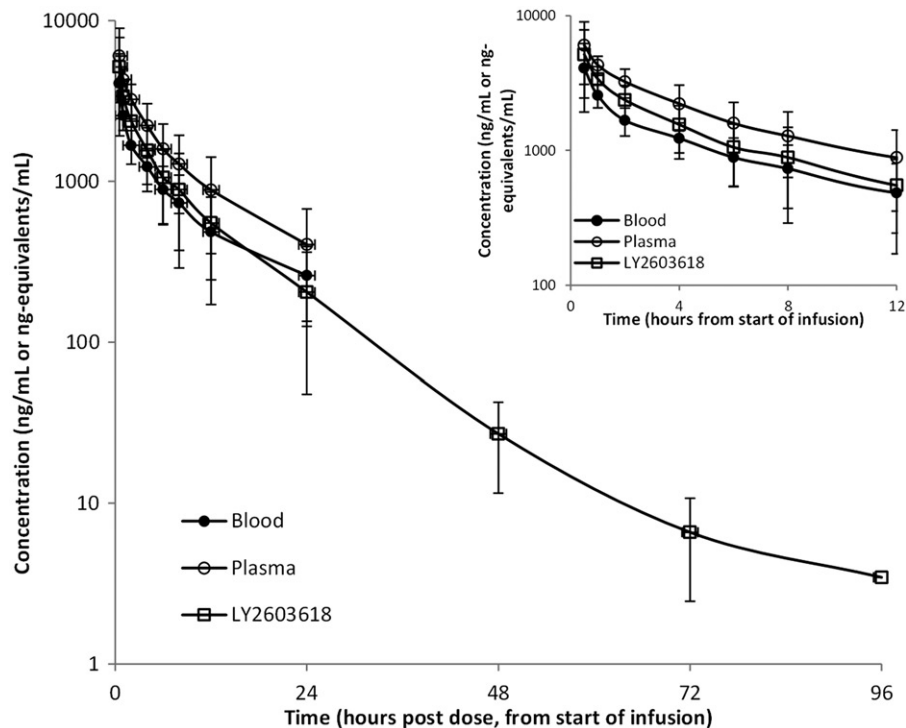


Table 2. Geometric mean (CV%) pharmacokinetic parameters of LY2603618 in plasma and total radioactivity in plasma and whole blood following a single IV administration of [14 C]LY2603618 to patients ($N=3$).

Parameter	Plasma LY2603618 ($N=3$)	Plasma total radioactivity ($N=3$)	Whole blood total radioactivity ($N=3$)
AUC(0– t_{last}) (ng·h/mL) ^a	22 200 (48)	27 700 (56)	15 700 (53)
AUC(0– ∞) (ng·h/mL) ^a	22 300 (48)	32 500 (63)	18 600 (59)
%AUC($t_{\text{last}}-\infty$) ^a	0.236 (8)	13.7 (46)	14.8 (33)
C_{max} (ng/mL) ^b	4750 (52)	5660 (47)	3740 (52)
t_{max} (h) ^c	0.48 (0.47–1.12)	0.48 (0.47–1.12)	0.48 (0.47–0.62)
t_{last} (h) ^c	71.6 (70.9–96.3)	23.9 (10.1–24.2)	23.9 (10.1–24.2)
$t_{1/2}$ (h) ^d	10.5 (8.5–12.4)	6.7 (2.8–10.6)	6.9 (3.1–10.9)
CL (L/h)	11.1 (47)	NC	NC
V_z (L)	168 (66)	NC	NC

AUC(0– ∞) = area under the concentration time curve from zero to infinity; AUC(0– t_{last}) = area under the concentration time curve from time zero to time t , where t is the last time point with a measurable concentration; %AUC($t_{\text{last}}-\infty$) = fraction of AUC(0– ∞) extrapolated from t_{last} to infinity; CL = total body clearance of drug (LY2603618 only) calculated after IV administration; C_{max} = maximum observed drug concentration; CV = coefficient of variation; N = number of patients; NC = not calculated; $t_{1/2}$ = apparent plasma terminal elimination half life; t_{last} = last time point where the concentration is above the limit of quantitation; t_{max} = time of maximum observed drug concentration; V_z = volume of distribution during the terminal phase (LY2603618 only).

^aRadioactivity units are ng equivalents/h/mL.

^bRadioactivity units are ng equivalents/mL.

^cMedian (range) data.

^dGeometric mean (range) data – calculated based on 0–24 h for blood and plasma radioactivity and 0–96 h for LY2603618

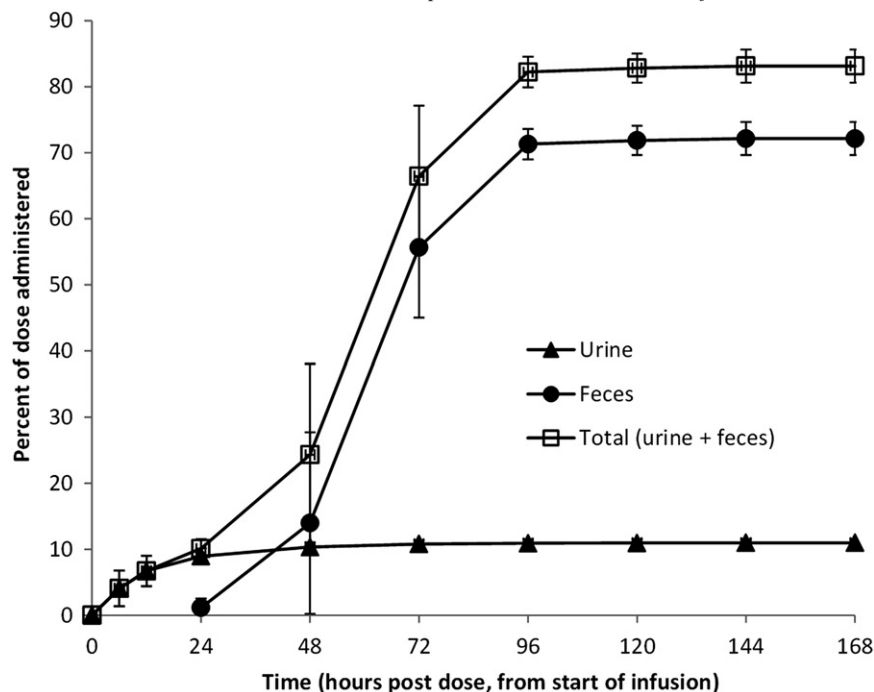
The first patient had the 1-h PK sample (scheduled prior to end of infusion, <5 minutes) collected 15 min late on Day 1/Cycle 1. The second patient vomited at 09:30 which resulted in a delay of 5 min for the 1-h PK and metabolism sample (scheduled prior to end of infusion, <5 min) collection on Day 1/Cycle 1. The third patient had 1-h PK and metabolite samples (scheduled prior to end of infusion, <5 min) collected 10 min late on Day 1/Cycle 1.

The mean plasma concentration versus time profiles for LY2603618 and total radioactivity in plasma and whole blood following IV administration of 250-mg (50- μ Ci) dose of [14 C]LY2603618 are depicted in Figure 1. The PK parameters of LY2603618, plasma total radioactivity, and whole blood total radioactivity following IV administration of 250-mg

(50- μ Ci) dose of [14 C]LY2603618 are tabulated in Table 2. The maximum plasma concentrations of LY2603618 (C_{max}) appeared to be attained at approximately 0.5 h (t_{max}) after the start of infusion. The geometric mean $t_{1/2}$ of LY2603618 was 10.5 h, with values for individual subjects ranging from 8.5 to 12.4 h (Table 2). Overall, LY2603618 was quantifiable in plasma samples up to approximately 72 h after the start of infusion in two patients and approximately 96 h in one patient.

Maximal levels of total radioactivity in plasma and whole blood were attained at a similar time to LY2603618 in plasma, with median t_{max} of approximately 0.5 h after the start of infusion for both matrices. Due to limitations in assay sensitivity, total radioactivity in plasma and blood were quantifiable only up to approximately 24 h, in all three

Figure 2. Arithmetic mean (\pm SD) cumulative percent recovery of radioactivity in urine and feces at specified intervals following a single IV administration of [14 C]LY2603618 to patients ($N=3$).



patients. Within this period, plasma concentrations of total radioactivity declined with a mean $t_{1/2}$ of 6.7 h, with individual estimates ranging from 2.8 to 10.6 h, and the whole blood concentrations of total radioactivity declined with a mean $t_{1/2}$ of 6.9 h, with individual estimates ranging from 3.1 to 10.9 h (Table 2).

The mean ratio of plasma concentrations of LY2603618 to plasma total radioactivity ranged from 0.640 to 0.844 through 12 h after the start of the infusion. The mean exposure to LY2603618, based on $AUC(0-\infty)$ and C_{max} , accounted for 68.7% and 83.9% of total radioactivity, respectively. The mean ratio of total radioactivity in whole blood to total radioactivity in plasma ranged from 0.515 to 0.666 through 12 h post-dose. The mean ratios of $AUC(0-\infty)$ and C_{max} for total radioactivity in whole blood to plasma were 0.57 and 0.66, respectively.

The between-patient variability in exposure to LY2603618 in plasma was high, with the geometric mean coefficient of variation (CV%) for $AUC(0-\infty)$ and C_{max} being 48 and 52%, respectively (Table 2). The variability in total radioactivity in plasma and whole blood was similar to LY2603618 (Table 2).

Excretion and mass balance in urine and feces

The cumulative excretion of total radioactivity in urine and feces up to 168 h post-dose is summarized in Figure 2. The percentages were calculated based on the theoretical nominal dose of [14 C]LY2603618 administered. The overall mean (\pm SD) recovery of total radioactivity in urine and feces samples was 83.14% (\pm 2.15%) during the study, with recoveries in individual patients ranging from 80.84% to 85.10%. A mean (\pm SD) of 72.16% (\pm 2.52%) of the dose was excreted in feces and 10.99% (\pm 0.57%) was excreted in urine up to the last collection interval. More than 65% of the administered radioactivity was recovered in the first 72 h post-dose. Total daily radioactivity excretion had declined to less

than 1% by the 96- to 120-h collection period. The total radioactivity expired into air for the three patients was approximately 0.2, 1.6 and 0.1% of the total dose, respectively.

Metabolism

Parent drug and 12 metabolites were tentatively identified in human plasma, urine and feces following a single 250-mg (50 μ Ci) IV infusion of [14 C]LY2603618. The proposed structures and the corresponding metabolite scheme are presented in Figure 3. Representative radioprofiles of plasma, feces and urine are shown in Figures 4–6. Relative percentages of metabolites quantified in plasma are shown in Table 3, and the percent dose of metabolites excreted in feces and urine are presented in Table 4. Radioprofiling of plasma from 1, 2, 4, 8 and 24 h revealed the presence of parent drug and 5 metabolites (by radioactivity and LC–MS). Parent drug was the most abundant radioactive peak, accounting for 72–77% of the circulating radioactivity across the profiled time points, followed by metabolites H2 and H5. Other less abundant metabolites included H8 (N-formylation on the morpholine nitrogen), H3 (mono-oxidation on the methyl group of the methylpyrazine ring), and H9 (oxidation on the pyrazine ring and oxidation on the pyrazine methyl group).

The relative AUC exposure of circulating metabolites to total circulating radioactivity was calculated using both the mean relative AUC values and the AUC pooling method (Hamilton et al., 1981; Hop et al., 1998). The first approach calculated AUC values based on the radioprofiles of the individual plasma time points across the reported time course. AUC values for parent and metabolites were determined using the concentrations (ng equivalents/mL) of parent and metabolites based on the total radioequivalents in plasma and the relative % radioactivity in the plasma time point for the

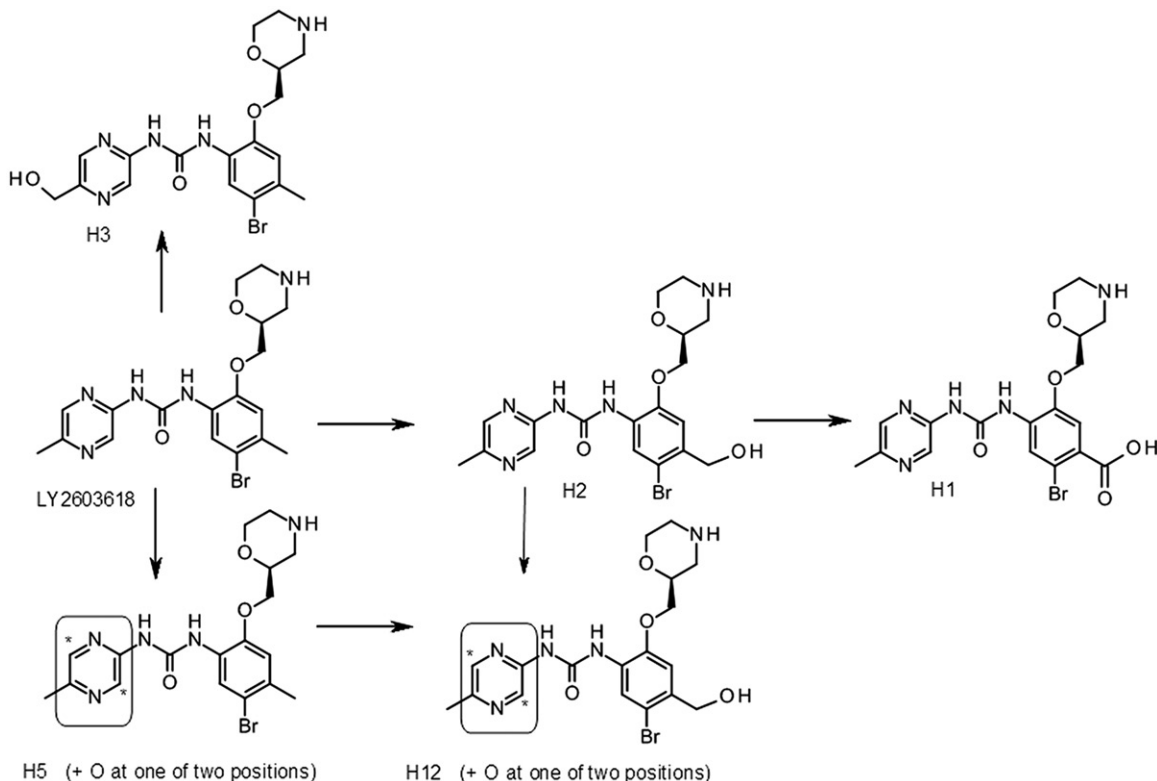
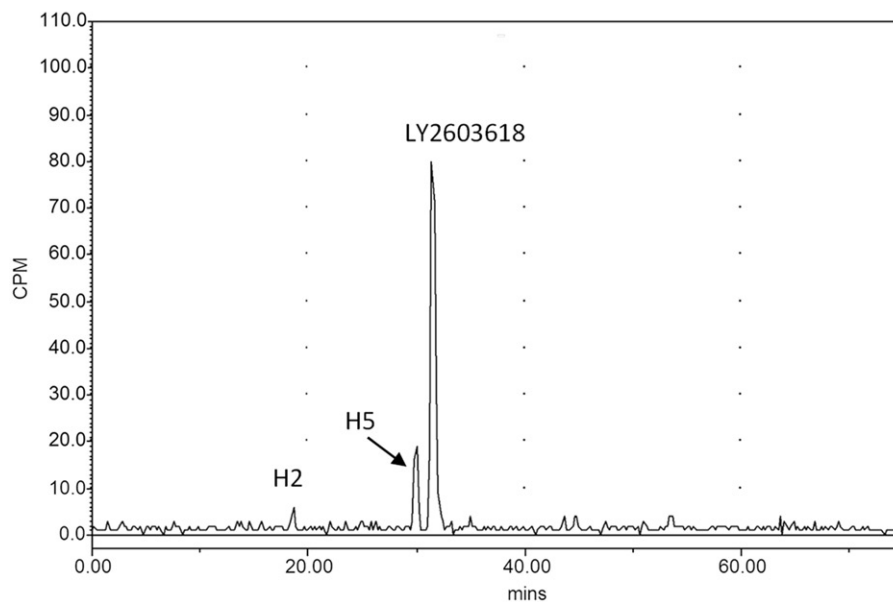


Figure 3. Major metabolic pathways of LY2603618 in human.

Figure 4. Representative radiochromatogram corresponding to pooled plasma from 0 to 24 h following a 1-h IV administration of radiolabelled LY2603618.



corresponding metabolites. These concentrations were then used to calculate AUC values for parent and relevant metabolites. Using this method, the mean relative AUC values of parent, H2 and H5 relative to total circulating radioactivity were 64% (range 62–65%), 5% (range 1–12%) and 7% (range <1 to 11%), respectively (Table 3). The second method used the plasma AUC pooling method (Hop et al., 1998). AUC pools were generated for each patient and exposure of parent and relevant metabolites were estimated relative to total circulating radioactivity. The mean relative AUC values of parent, H2 and H5 relative to total circulating

radioactivity were 73% (range 67–80%), 6% (range <1 to 9%) and 9% (range <1 to 15%), respectively, using the AUC pools (Table 3). Both of these methods provided estimates of metabolite exposures relative to total circulating radioactivity and demonstrated comparable mean exposure estimates for H2 and H5.

Only the parent drug and one metabolite (H2) were identified in the urine collected from 0 to 24 h. Parent drug accounted for approximately 2–5% of the administered dose whereas metabolite H2 represented approximately 3–4% of the administered dose eliminated in urine.

Figure 5. Radiochromatogram representing 24–72 h fecal extract following a 1-h IV administration of radiolabelled LY2603618.

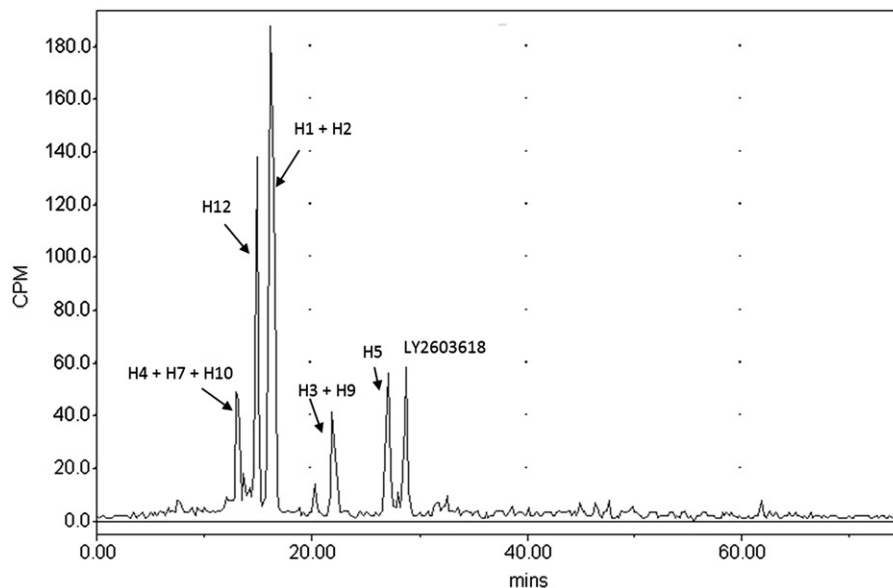
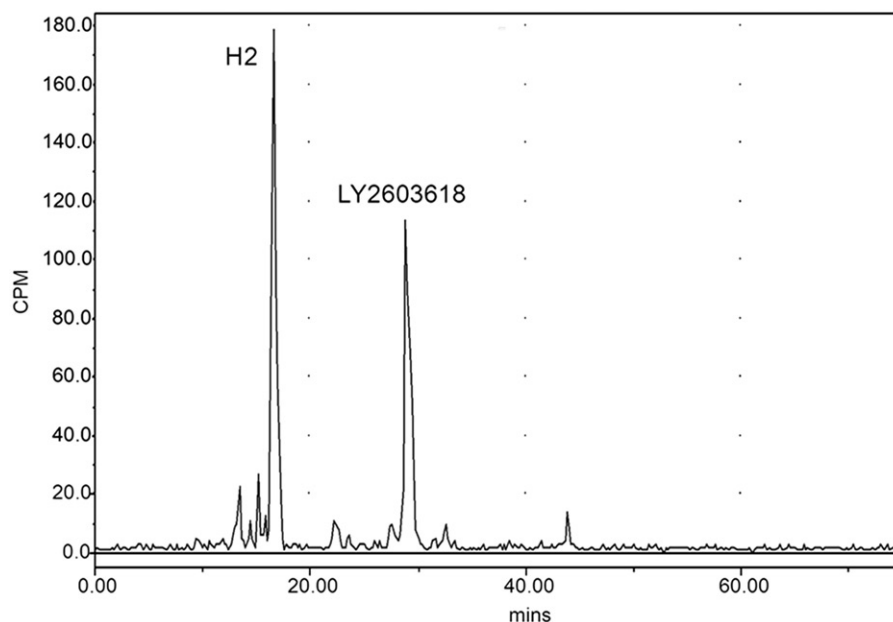


Figure 6. Radiochromatogram representing 0–24 h urine following a 1-h IV administration of radiolabelled LY2603618.



Radioprofiling of feces from 24 to 96 h revealed parent drug and 11 metabolites. The 0–24 h time period was not profiled due to low radioactive counts. LY2603618 represented approximately 6% of the administered dose, whereas H2 was the largest metabolite (~22% of the dose) in the feces followed by H12 (9% of the dose), H1 (8% of the dose), H5 (5% of the dose) and minor metabolites H6 and H11 (each <5% of the dose). Metabolites H7 + H4 + H10 co-eluted and accounted for 11% of the dose while H3 + H9 co-eluted accounting for approximately 6% of the dose. Overall, the metabolic profiles were comparable across patients.

LC-MS/MS fragmentation of LY2603618

LC-MS/MS with accurate mass measurement were utilized for the identification of LY2603618 and metabolites.

The molecular ions and characteristic product ions for LY2603618 and metabolites found in plasma, urine and feces are shown in Table 5.

LY2603618

The accurate mass protonated molecular ion ($[M + H]^+$) was observed at m/z 436.0977, consistent with the following chemical formula: $C_{18}H_{23}BrN_5O_3$. The following product ions were used in the characterization of the structure: m/z 327 (loss of 2-amino-5-methylpyrazine), m/z 301 (loss of 5-methylpyrazine isocyanate), m/z 240 (3-bromo-4-methyl-5-propenyl-6-hydroxyaniline cation), m/z 222 (loss of Br radical from m/z 301), m/z 210 (loss of formaldehyde from m/z 240), m/z 161 (loss of Br radical from m/z 240), m/z 136 ($[M + H]^+$ of 4-methylpyrazine isocyanate), m/z 123 (2-hydroxy-4-methylaniline radical cation), m/z 110 ($[M + H]^+$ of

Table 3. Mean relative exposure of circulating metabolites in plasma based on individual time points and AUC pools following the administration of a single radiolabelled dose of LY2603618.

	Patient Number			Mean ^d	Range
	1001	1002	1003		
Individual time points	0–24 h	0–24 h	0–8 h		
Total radioactivity	100%	100%	100%	100%	100%
Parent	65%	65%	62%	64%	62–65%
H2	1%	3%	12%	5%	1–12%
H5	11%	11%	NQ ^e	7% ^d	NQ–11%
AUC last total radioactivity ^a	44265	31447	14092		
	Time points				
%AUC pool ^c	0–24 h	0–8 h ^b	0–8 h	Mean	Range
Parent	71%	80%	67%	73%	67–80%
H2	NQ	8%	9%	6% ^d	NQ–9%
H5	15%	11%	NQ	9% ^d	NQ–15%

NQ = not quantifiable (<7 cpm in peak height) or not detected.

^aAUC last total radioactivity values were calculated in WinNonlin version 5.3 using an oral dose model.

^b%AUC pool sample for Patient 1002 pooled plasma from 1 to 8 h instead of 1–24 h due to volume constraints.

^c%AUC pool values were corrected for extraction recoveries.

^d*n* = 3. NQ assigned value of zero.

^eH5 was detected by LC-MS only in a 1, 2 and 4 h pooled sample.

Table 4. Summary of metabolites excreted in feces and urine following a single radiolabelled dose of LY2603618 expressed as percentage of dose.

Metabolite	Percent dose (Mean, <i>N</i> = 3)		
	Urine	Feces	Total
P	3.3	5.6	8.9
H1 ^b	NQ	8.0	8.0
H2 ^b	3.0	21.7	24.7
H6	NQ	0.4	0.4
H12	NQ	8.7	8.7
H5	NQ	4.9	4.9
H11	NQ	0.6	0.6
H7 + H4 + H10	NQ	10.6	10.6
H3 + H9	NQ	6.3	6.3
Total % Identified	6.3	66.8	73.1
% Dose Eliminated ^a	11.0	70.2	81.2

NQ = not quantifiable or not detected.

^a% dose eliminated in samples profiled 0–24 h urine and 24–96 h feces.

^b% dose values for H1 and H2 were obtained from a secondary chromatographic separation.

2-amino-5-methylpyrazine), *m/z* 100 (2-methylmorpholine cation) and *m/z* 98 [observed in MS3 scan of *m/z* 301 – 2-methylmorpholine cation (–2H)].

NMR identification of H2 and H3

LY2603618

The full proton and carbon chemical shift assignments are shown in Table 6. The NMR spectrum of parent was used to facilitate interpretation of the NMR spectra of H2 and H3.

Metabolite H2

The full proton and carbon chemical shift assignments, and the correlations used to define the structure are shown in Table 6. A new methylene (compared with parent) was

observed in the HSQC at 4.62/64.2 ppm for the proton/carbon pair and is consistent with a hydroxylated methylene. The HMBC correlations from the 18-methylene (substituent to the bromobenzene) to the 14-, 15- and 16-carbons clearly identify 18-methylene as the location of the hydroxylated methylene.

Metabolite H3

The full proton and carbon chemical shift assignments and the correlations used to define the structure are shown in Table 6. A new methylene (compared to parent) was observed in the HSQC at 4.70/64.1 ppm for the proton/carbon pair and is consistent with a hydroxylated methylene. The gCOSY correlations from the 7-methylene (substituent to the pyrazine) to H3 clearly identify it as the location of the hydroxylated methylene. This correlation was also observed in the parent for H3 to the 7-methyl group.

Identification of P450s involved in the clearance of LY2603618

In the initial screening experiment, LY2603618 was incubated with a panel of recombinant P450s to measure substrate depletion. Recombinant P450s rCYP 1A2, rCYP2B6, rCYP2C8, rCYP2C9, rCYP2C19, rCYP2E1, rCYP2J2 and rCYP3A5 did not contribute to the depletion of LY2603618. rCYP2D6 and rCYP3A4 met all criteria for signals indicating participation in clearance of LY2603618. Incubation conditions for rCYP3A4 were further optimized to ensure initial rate conditions, and the results of the RAF-based scaling showed that rCYP3A4 was responsible for approximately 95% of the P450-mediated clearance of LY2603618, while the remaining 5% was CYP2D6 mediated (Table 7).

Involvement of AO in the formation of H5

LY2603618 mono-oxidized metabolite H5 was only detected in cytosol from monkey and human liver and was tentatively identified based on its product ion spectrum and retention relative to parent, which were consistent with those observed in the clinical plasma and feces samples. To further confirm that H5 formation is catalyzed by AO, LY2603618 was co-incubated with hydralazine, an AO inhibitor, in human liver cytosol. H5 was not detected in the incubations that contained hydralazine.

Conservative estimate of magnitude of potential DDI

$F_{e,parent}$ and $F_{m,AO}$ are presented in Table 4 as total percentage dose identified as parent (P) and H5, respectively, divided by 100. Thus, F_{m,all_CYPs} was estimated at 0.86 [Equation (2)] and the magnitude of DDI upon complete inhibition of CYP-mediated clearance, expressed as AUC_i/AUC [AUC ratio; Equation (3)], was estimated to be 7.1. Based on the $f_{m,CYP2D6}$ and $f_{m,CYP3A}$ determined *in vitro*, CYP3A inhibitors would be expected to have a much larger effect on exposure to LY2603618 than CYP2D6 inhibitors.

Discussion

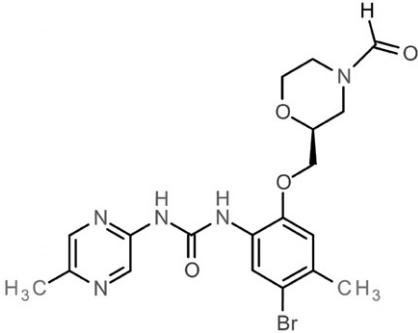
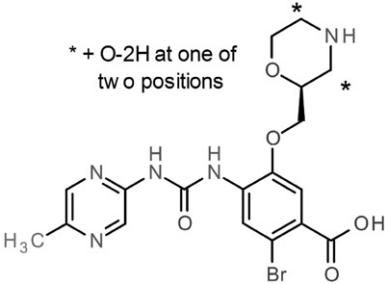
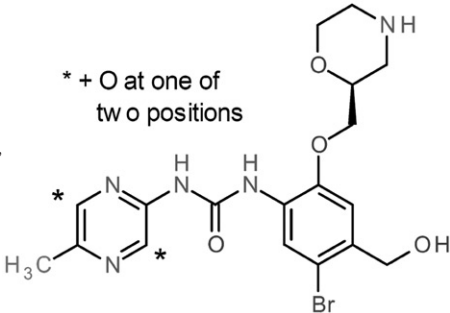
The objective of this study was to determine the disposition and metabolism of LY2603618 in patients with advanced and/or metastatic solid tumors following an IV administration of a

Table 5. LC-MS/MS and chemical structures for LY2603618 and metabolites detected.

Metabolite ID, Occurrence	Proposed Chemical Structure	Metabolite ID, Occurrence	Proposed Chemical Structure
Parent $[M + H]^+$: 436 MM: 436.0977 TM: 436.0979 F: $C_{18}H_{23}BrN_5O_3$ Δ ppm: -0.4 CPI (m/z): 327, 301, 240, 222, 210, 161, 136 , 123, 110, 100, 98 (MS ³ scan of m/z 301)		H3 $[M + H]^+$: 452 MM: 452.0929 TM: 452.0928 F: $C_{18}H_{23}BrN_5O_4$ Δ ppm: 0.2 CPI (m/z): 327, 301, 240, 222, 161, 152 , 126, 100	
H1 $[M + H]^+$: 466 MM: 466.0715 TM: 466.0721 F: $C_{18}H_{21}BrN_5O_5$ Δ ppm: -1.2 CPI (m/z): 357, 339, 331, 313 , 214, 136, 110, 100 MS ³ (m/z 331): 313, 287, 213, 100		H4 $[M + H]^+$: 344 MM: 344.0606 TM: 344.0604 F: $C_{13}H_{19}BrN_3O_3$ Δ ppm: 0.5 CPI (m/z): 327, 301 , 240, 222, 210, 161, 123, 100	
H2 $[M + H]^+$: 452 MM: 452.0927 TM: 452.0928 F: $C_{18}H_{23}BrN_5O_4$ Δ ppm: -0.2 CPI (m/z): 343, 325, 317, 299 , 240, 238, 200, 136, 110, 100, 98 (MS ³ scan of m/z 317)		H5 $[M + H]^+$: 452 MM: 452.0925 TM: 452.0928 F: $C_{18}H_{23}BrN_5O_4$ Δ ppm: -0.7 CPI (m/z): 327 , 301, 240, 222, 152, 126, 100	
H6 $[M + H]^+$: 466 MM: 466.0719 TM: 466.0721 F: $C_{18}H_{21}BrN_5O_5$ Δ ppm: -0.3 CPI (m/z): 313 , 296, 295, 268, 234, 200, 136, 110, 86		H9 $[M + H]^+$: 468 MM: 468.0874 TM: 468.0877 F: $C_{18}H_{23}BrN_5O_5$ Δ ppm: -0.7 CPI (m/z): 327 , 301, 248, 168, 142, 124, 100	
H7 $[M + H]^+$: 468 MM: 468.0875 TM: 468.0877 F: $C_{18}H_{23}BrN_5O_5$ Δ ppm: -0.4 CPI (m/z): 343, 325, 299, 240, 200, 152 , 126, 100		H10 $[M + H]^+$: 484 MM: 484.0826 TM: 484.0826 F: $C_{18}H_{23}BrN_5O_6$ Δ ppm: -0.1 CPI (m/z): 343, 325, 299, 168 , 142 , 124, 100	
H8 $[M + H]^+$: 464 MM: 464.0925 TM: 464.0928 F: $C_{19}H_{23}BrN_5O_4$ Δ ppm: -0.6		H11 $[M + H]^+$: 480 MM: 480.0511 TM: 480.0513 F: $C_{18}H_{19}BrN_5O_6$ Δ ppm: -0.5	

(continued)

Table 5. Continued

Metabolite ID, Occurrence	Proposed Chemical Structure	Metabolite ID, Occurrence	Proposed Chemical Structure
CPI (<i>m/z</i>): 329, 301, 250 , 136, 128, 110, 100		CPI (<i>m/z</i>): 327, 240, 214, 136 , 110	
H12 [M + H] ⁺ : 468 MM: 468.0875 TM: 468.0877 F: C ₁₈ H ₂₃ BrN ₅ O ₅ Δ ppm: -0.4 CPI (<i>m/z</i>): 343, 325, 317, 299, 200, 152, 126 , 100			

MM = measured mass; TM = theoretical mass; F = formula; Δ ppm = (mDa/theoretical mass) × 100; CPI (*m/z*) = characteristics product ions (*m/z*).
Note: Bolded ion represents the predominant ion in the spectrum.

250-mg (50 μCi) dose of [¹⁴C]LY2603618. The study was conducted at a single-centre and enrolled patients with advanced or metastatic solid tumors for whom standard of care was refractory and/or no standard of care existed. Patients received LY2603618 in combination with gemcitabine subsequent to the radiolabelled dose. Since LY2603618 was classified as a cytostatic and had to be given to cancer patients, enrolment was on a rolling basis. As the study progressed, it became apparent that enrolling patients with advanced stages of cancer was more challenging than expected due to the required length of stay in the clinic (up to 7 days). Extension of the enrolment period, which was on a rolling basis, required the establishment of extended stability for the ¹⁴C drug product. Establishment of such stability data is typically not required when conducting ¹⁴C labelled disposition studies conducted in healthy volunteers because all of the volunteers are dosed on the same day.

Approximately 6 months into the study, the protocol was amended to reduce the CRU stay to a maximum of 4 days, supported by the fact that greater than 80% of radioactivity from the first two patients was eliminated by 96 h. The duration between enrolment of the first patient and the third patient was approximately 10 months, which illustrates the challenge of enrolling oncology patients in radiolabelled disposition studies. Subsequently, a decision was made following the third patient completing the study that the ongoing review of the data from the three patients was deemed acceptable and sufficient to meet the study objectives and the study was closed. Long-term stability was

successfully established for the [¹⁴C]LY2603618 drug product covering the period from the date of manufacture to the date the last patient was dosed.

An average of 83% of the radioactive dose was recovered from the three patients. Although recoveries of >90% are desired from disposition studies (Roffey et al., 2007), lower recoveries and high variability have been routinely reported from oncology patients (Beumer et al., 2005, 2007; Jost et al., 2006). Overall, biliary-fecal excretion of radioactivity was the primary route of elimination with a mean of 72% of radioactivity eliminated in feces, 11% in urine and a negligible amount (0.1–1.6%) in expired air. Radioactivity was rapidly excreted since 65% of radioactivity was recovered within 72 h. LY2603618 and 12 metabolites were identified in human plasma, urine and feces following a single IV dose of [¹⁴C]LY2603618.

Total radioactivity in plasma and whole blood were quantifiable over a shorter period than plasma concentrations of LY2603618 due to differences in assay sensitivity. Therefore, the *t*_{1/2} estimates for radioactivity may not be a true representation of the terminal elimination phase for total radioactivity in plasma and whole blood. However, as depicted in Figure 1 inset, the PK profiles of LY2603618 and radioactivity were comparable out to 12 h.

The mean ratios of AUC(0–∞) and C_{max} for total radioactivity in whole blood to plasma were 0.57 and 0.66, respectively, suggesting a low association of LY2603618-related material to blood cells. When combined with the mean hematocrit values of approximately 30%, this suggests that

Table 6. NMR data for LY2603618, H2 and H3.

Shift assignments of LY2603618 in CD ₃ OD				Shift assignments of LY2603618 metabolite H2 in CD ₃ OD				Shift assignments of LY2603618 metabolite H3 in CD ₃ OD			
Atom	¹ H, ppm	¹³ C, ppm	Multiplicity, Hz	¹ H, ppm	¹³ C, ppm	Multiplicity, Hz	¹ H, ppm	¹³ C, ppm	Multiplicity, Hz		
2	—	147.71	—	—	147.13	—	8.45	139.92	s		
3	8.22	141.23	s	8.24	140.87	s	—	—	—		
5	—	149.19	—	—	148.66	—	8.49	135.31	br. s.		
6	8.49	135.27	s	8.55	134.62	s	4.70	64.05	s		
7	2.50	20.50	s	2.49	19.95	s	—	—	—		
12	—	128.72	—	—	129.27	—	—	—	—		
13	—	148.85	—	—	148.27	—	6.98	115.21	s		
14	6.99	115.57	s	7.21	112.42	s	—	—	—		
15	—	134.00	—	—	135.88	—	—	—	—		
16	—	116.86	—	—	113.41	—	—	—	—		
17	8.36	124.84	s	8.43	124.04	s	8.42	124.42	s		
18	2.34	22.95	s	4.62	64.19	s	2.35	22.88	s		
21	4.15	71.21	m	—	—	—	4.11	71.52	m		
21''	—	—	—	4.19	70.77	m	—	—	—		
21'	—	—	—	4.13	70.90	m	—	—	—		
22	4.07	74.84	m	4.03	75.25	m	4.02	76.05	m		
24''	4.03	66.85	m	3.94	67.52	m	3.96	68.09	m		
24'	3.79	66.83	td (<i>J</i> = 12 × (2), 2.6)	3.72	67.55	m	3.74	68.14	m		
25''	3.06	45.37	m	2.76	50.01	m	2.76	50.53	m		
25'	3.00	45.37	m	2.69	50.05	m	2.69	50.55	m		
27''	3.27	47.16	d (<i>J</i> = 12.1)	3.02	52.49	m	3.01	52.86	m		
27'	2.92	47.14	m	2.55	52.47	m	2.55	52.87	m		

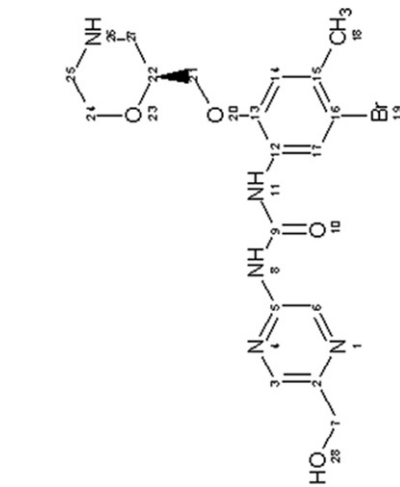
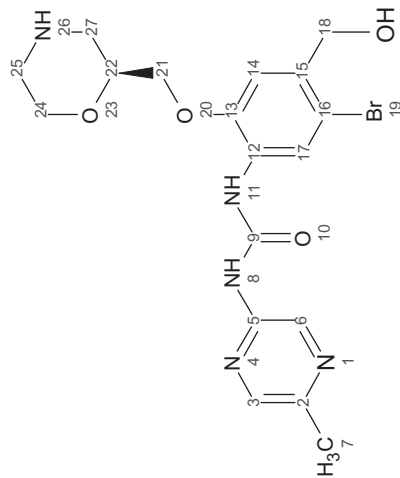
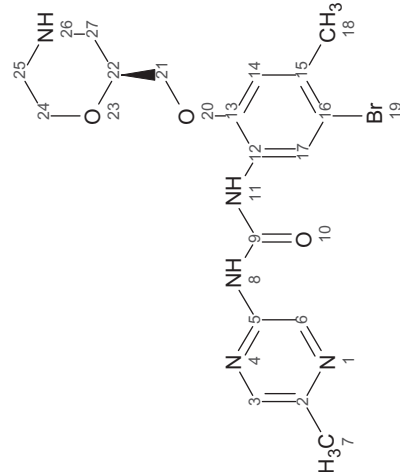


Table 7. Scaling of recombinant P450 CL_{int} of LY2603618 as determined by LY2603618 depletion to predict f_{mCYP}.

CYP	-k (min ⁻¹)	Incubation protein concentration (mg mL ⁻¹)	CL _{int} (μL min ⁻¹ mg ⁻¹)	rCYP Content (pmol mg ⁻¹)	CL _{int} ⁻¹ (μL min ⁻¹ pmol CYP ⁻¹)	RAF (pmol CYP mg ⁻¹)	Scaled CL _{int} , HLM (μL min ⁻¹ mg ⁻¹)	f _{mCYP}
CYP2D6	0.0658	0.25	263	83	3.2	0.573	1.8	0.05
CYP3A4	0.0306	0.25	122	147	0.83	43.7	36	0.95

k = depletion rate constant; CL_{int} = intrinsic clearance; rCYP = recombinant CYP; RAF = relative activity factor; f_{mCYP} = fraction metabolized by a particular CYP.

LY2603618-related material undergoes minimal distribution to the blood cell compartment. The mean exposure to LY2603618, based on AUC(0–∞), accounted for 68.7% of the total radioactivity, suggesting that LY2603618 was the major circulating entity along with minor circulating metabolite(s). Radioprofiling of plasma confirmed the radio-PK results and indicated that parent was the largest circulating drug related component at all time points profiled across patients and in the AUC plasma pools.

In addition to parent drug, five relatively minor metabolites were detected in plasma, of which only two metabolites (H2 and H5) were quantifiable for relative AUC calculations. Relative AUC calculations indicated that H2 and H5 represented <10% of the circulating total radioactivity; however, H5 was a unique human/non-human primate metabolite not previously reported in the rat or dog (unpublished data). LC–MS/MS suggested that metabolite H2 resulted from mono-oxidation of the methyl group on the bromobenzyl ring. A key fragment ion in the spectrum was the ion at 200 m/z, the 2-amino-4-bromo-5-hydroxybenzyl cation (Table 5).

NMR experiments confirmed the LC–MS/MS assignment of H2 showing a new methylene proton (compared to parent), at 4.62/64.2 ppm for the proton/carbon pair in the HSQC spectrum (Table 6). Metabolite H5 was unique to human and non-human primate, and was identified *in vitro* in human and non-human primate microsomes/cytosol, and *in vivo* in human. The LC–MS/MS spectrum showed diagnostic product ions at 327 m/z (the [5-bromo-4-methyl-2-[[[(2S)-morpholin-2-yl]methoxy]anilino]methanone acylium ion and 126 m/z [3-hydroxy-5-methyl-pyrazin-2-yl]ammonium ion) lack of water loss suggested that oxidation had occurred on the pyrazine moiety and not the methyl group (Table 5). Attempts were unsuccessful to scale-up H5 for NMR.

It was speculated that AO could be involved in the formation of H5. This hypothesis was further supported by the apparent species specificity in the formation of H5. AO is a molybdenum cofactor-containing soluble enzyme found in the liver and other mammalian tissues that oxidizes carbon atoms on aromatic azaheterocyclic compounds. AO is either variably expressed or not expressed at all in common laboratory species (rat or dog); however, AO is highly expressed in monkey and human (Beedham, 2002). Results following the incubation with rat, dog, monkey and human cytosol confirmed that H5 was only generated in the human and monkey, consistent with the species specificity of AO. Further confirmation that H5 was formed via AO was demonstrated by the complete inhibition of H5 formation by hydralazine, an AO inhibitor (Zientek et al., 2010). Therefore, the

identity of H5 was confirmed as a metabolite formed by AO with oxidation on one of the two pyrazine aromatic carbon atoms.

Metabolite profiling of feces and urine revealed that <10% of LY2603618 was recovered intact, indicating LY2603618 was extensively metabolized in humans. The radioprofiles of feces and urine were similar across all three patients. Metabolite H1 showed the protonated molecular ion at 466 m/z consistent with an addition of 2O and loss of 2H from the parent. In the MS–MS spectrum key fragment ions included 214 m/z the 2-bromo-4-amino-5-hydroxybenzyl acylium ion, and the loss of CO₂ from the 331 m/z ion to give 287 m/z was consistent with the formation of a carboxylic on the bromobenzyl methyl group (Table 5). Metabolite H12 showed the protonated molecular ion at 468 m/z consistent with the addition of 2 oxygen atoms to the parent. LC–MS/MS revealed the diagnostic product ions 200 m/z, the 2-amino-4-bromo-5-hydroxybenzyl cation and 126 m/z, the [5-(hydroxymethyl)pyrazin-2-yl] ammonium ion, indicating oxidation on the bromobenzyl methyl group and the pyrazine moiety (Table 5). Metabolite H5 represented approximately 5% of the dose in feces. The remaining metabolites in feces were either minor (<1% of the dose) or co-eluted and were not separable using the current chromatographic methods. Metabolite H3 (which co-eluted with H9) gave a protonated molecular ion at 452 m/z, resulting from mono-oxidation. LC–MS/MS of metabolite H3 showed a diagnostic fragment ion at 126 m/z, a [5-(hydroxymethyl)pyrazin-2-yl]ammonium ion, indicating oxidation on the pyrazine moiety. NMR experiments refuted the initial LC–MS/MS assignment, showing a new methylene proton (compared to parent) at 4.70/64.1 ppm for the proton/carbon pair in the HSQC spectrum (Table 6). These data confirm that hydroxylation has occurred on the pyrazine ring methyl group.

Conclusions

The major metabolic clearance pathway is via CYP450s which accounted for approximately 60% of the quantified metabolites recovered in feces and urine. In addition, formation of H5 via AO was responsible for approximately 5% of the administered dose. M5 appears to be unique to human and non-human primate, however in the clinical development of this compound the rat and dog were used for toxicological testing. It remains uncertain if additional toxicological testing of M5 will be required. Metabolite H2 (hydroxylated methylene) was the largest metabolite

formed and represented approximately 25% of the administered dose. Approximately 6% of the parent was excreted unchanged in the feces and approximately 3% in the urine.

The data represented here demonstrate the involvement of multiple metabolic clearance pathways for LY2603618 following the administration of a 250-mg dose via IV administration to patients with cancer. The clearance pathways are in agreement with the Biopharmaceutics Drug Disposition Classification System proposed by Wu & Benet (2005), since LY2603618 is classified as “class 2”.

Results from substrate depletion analysis using a panel of recombinant P450s indicated that CYP3A4 was predominantly responsible for P450 mediated metabolism of LY2603618, with a minor contribution from CYP2D6. Therefore, co-administration of a strong CYP3A inhibitor could result in a significant increase in LY2603618 exposures and would need to be further evaluated. In general, the involvement of multiple P450 and non-P450 clearance pathways could be advantageous with respect to reducing the potential for clinical drug–drug interactions. The lack of dependency on a single metabolic route is especially important in patients with cancer who are frequently taking many medications both to treat the underlying neoplasm, deal with the iatrogenic conditions produced and treat any concomitant disease process.

Overall, a single 250-mg (50- μ Ci) IV dose of [¹⁴C]LY2603618 was generally well tolerated in patients. There were no clinically significant adverse events. However, LY2603618 given in combination with gemcitabine during the extension phase had more drug-related adverse events in these three patients. Two of the three patients had radiologically documented disease progression at follow-up. The third patient demonstrated a clinical progression, and no radiological documentation was determined to be necessary.

Patient enrolment was the main limitation during the conduct of this study. Enrolment was additionally hindered by the long in-patient stay required for complete sample collection. Adequate planning and execution of [¹⁴C]LY2603618 drug stability studies enabled patient enrolment and dosing over an extended period of time.

Acknowledgements

The authors would like to thank Chad Hadden, Ph.D. for NMR support, Boris Czeskis, Ph.D., for synthesis of [¹⁴C] labelled LY2603618, Amy Burdan and Elizabeth Wagner for editorial support, and William Ehlhardt, Ph.D. for critical review and insightful comments.

Declaration of interest

This work was supported by Eli Lilly and Company. Wickremsinhe, Hynes, Palmieri, Mitchell, Abraham, Rehmel, Chana and Cassidy are employees and shareholders of Eli Lilly and Co.

References

- Beedham C. (2002). Molybdenum hydroxylases. In: Ioannides C, ed. Enzyme systems that metabolise drugs and other xenobiotics. New York: John Wiley & Sons, 147–88.
- Beumer JH, Rademaker-Lakhai JM, Rosing H, et al. (2005). Trabectedin (Yondelis, formerly ET-743), a mass balance study in patients with advanced cancer. *Invest New Drugs* 23:429–36.
- Beumer JH, Garner RC, Cohen MB, et al. (2007). Human mass balance study of the novel anticancer agent ixabepilone using accelerator mass spectrometry. *Invest New Drugs* 25:327–34.
- Hamilton RA, Garnett WR, Kline BJ. (1981). Determination of mean valproic acid serum level by assay of a single pooled sample. *Clin Pharmacol Ther* 29:408–13.
- Hop CE, Wang Z, Chen Q, Kwei G. (1998). Plasma-pooling methods to increase throughput for in vivo pharmacokinetic screening. *J Pharm Sci* 87:901–3.
- Jost LM, Gschwind HP, Jalava T, et al. (2006). Metabolism and disposition of vatalanib (PTK787/ZK-222584) in cancer patients. *Drug Metab Dispos* 34:1817–28.
- King C, Diaz H, Darlene B, et al. (2014). Characterization and preclinical development of LY2603618: a selective and potent Chk1 inhibitor. *Invest New Drugs* 32:213–26.
- Matthews TP, Jones AM, Collins I. (2013). Structure-based design, discovery and development of checkpoint kinase inhibitors as potential anticancer therapies. *Expert Opin Drug Discov* 8:621–40.
- Nakajima M, Nakamura S, Tokudome S, et al. (1999). Azelastine N-demethylation by cytochrome P450 (CYP)3A4, CYP2D6, and CYP1A2 in human liver microsomes: evaluation of approach to predict contribution of multiple CYPs. *Drug Metab Dispos* 27:1381–91.
- Penner N, Klunk LJ, Prakash C. (2009). Human radiolabeled mass balance studies: objectives, utilities and limitations. *Biopharm Drug Dispos* 30:185–203.
- Rehmel JF, Heim J, Oluyedun O, et al. (2012) Poster P42: rapid and early identification of P450s involved in test article metabolism. *Drug Metab Rev* 44:36–152.
- Roffey SJ, Obach RS, Gedge JI, Smith DA. (2007). What is the objective of the mass balance study? A retrospective analysis of data in animal and human excretion studies employing radiolabeled drugs. *Drug Metab Rev* 39:17–43.
- Weiss GJ, Donehower RC, Iyengar T, et al. (2013). Phase I dose-escalation study to examine the safety and tolerability of LY2603618, a checkpoint 1 kinase inhibitor, administered 1 day after premetrexed 500mg/m(2) every 21 days in patients with cancer. *Invest New Drugs* 31:136–44.
- Wu CY, Benet LZ. (2005). Predicting drug disposition via application of BCS: transport/absorption/elimination interplay and development of a biopharmaceutics drug disposition classification system. *Pharm Res* 22:11–23.
- Zientek M, Jiang Y, Youdim K, Obach RS. (2010). In vitro-in vivo correlation for intrinsic clearance for drug metabolized by human aldehyde oxidase. *Drug Metab Dispos* 38:1322–7.